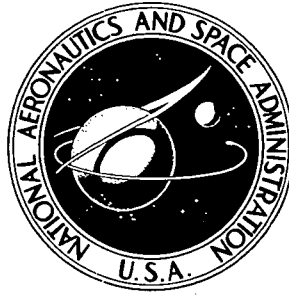


**NASA TECHNICAL
MEMORANDUM**



NASA TM X-3045

NASA TM X-3045

**CASE FILE
COPY**

**TWO-DIMENSIONAL COLD-AIR CASCADE STUDY
OF A FILM-COOLED TURBINE STATOR BLADE**

**I - Experimental Results of Pressure-Surface
Film Cooling Tests**

*by Thomas P. Moffitt, Herman W. Prust, Jr.,
and Wayne M. Bartlett*

*Lewis Research Center
Cleveland, Ohio 44135*



Page Intentionally Left Blank

1. Report No. NASA TM X -3045	2. Government Accession No.	3. Recipient's Catalog No.	
4. Title and Subtitle TWO-DIMENSIONAL COLD-AIR CASCADE STUDY OF A FILM-COOLED TURBINE STATOR BLADE I - EXPERIMENTAL RESULTS OF PRESSURE-SURFACE FILM COOLING TESTS		5. Report Date MAY 1974	6. Performing Organization Code
		8. Performing Organization Report No. E-7817	10. Work Unit No. 501-24
7. Author(s) Thomas P. Moffitt, Herman W. Prust, Jr., and Wayne M. Bartlett		11. Contract or Grant No.	
		13. Type of Report and Period Covered Technical Memorandum	
9. Performing Organization Name and Address Lewis Research Center National Aeronautics and Space Administration Cleveland, Ohio 44135		14. Sponsoring Agency Code	
		12. Sponsoring Agency Name and Address National Aeronautics and Space Administration Washington, D.C. 20546	
15. Supplementary Notes			
16. Abstract The effect of film coolant ejection from the pressure side of a stator blade was determined in a two-dimensional cascade. Stator exit surveys were made for each of six rows of coolant holes. Successive multirow tests were made with two, three, four, five, and six rows of coolant holes open. The results of the multirow tests are compared with the predicted multirow performance obtained by adding the single-row data. Results are presented in terms of stator primary-air efficiency as a function of coolant fraction.			
17. Key Words (Suggested by Author(s)) Turbine film-cooling Aerodynamics Cascades		18. Distribution Statement Unclassified - unlimited Category. 28	
19. Security Classif. (of this report) Unclassified	20. Security Classif. (of this page) Unclassified	21. No. of Pages 30	22. Price* \$3.25

* For sale by the National Technical Information Service, Springfield, Virginia 22151

Page Intentionally Left Blank

TWO-DIMENSIONAL COLD-AIR CASCADE STUDY OF A FILM-COOLED TURBINE STATOR BLADE

I - EXPERIMENTAL RESULTS OF PRESSURE-SURFACE FILM COOLING TESTS

by Thomas P. Moffitt, Herman W. Prust, Jr., and Wayne M. Bartlett

Lewis Research Center

SUMMARY

The influence on stator blade performance of coolant discharge from each of six individual rows of coolant holes on the pressure surface was determined experimentally in a two-dimensional cascade where the temperature of the coolant was equal to the primary-air inlet temperature. Multirow combinations of two, three, four, five, and six rows of holes were also tested. The results of the multirow tests were then compared with predicted multirow performance obtained by adding the results of the single-row tests.

For the blade tested, the change in primary efficiency was dependent primarily on the amount of coolant added and was essentially independent of the number or location of coolant holes and the Mach number.

A significant portion of the ideal energy of the coolant resulted in useful kinetic energy at the exit of the blade row. When the blade cavity pressure (coolant supply) was equal to the inlet pressure of the primary flow, about 80 percent of the ideal coolant energy was measured at the blade exit as a net increase in kinetic energy output.

The output energy from single-row holes is additive. Excellent agreement was obtained between measured multirow coolant ejection performance and predicted multirow performance obtained by adding measured single-row data. Apparently flow from a row of holes on the pressure surface did not affect the performance of coolant flow ejected from holes downstream on the pressure surface.

INTRODUCTION

Several analytical studies concerning the performance of cooled turbines (e. g. , refs. 1 and 2) have shown that different means of ejecting compressor bleed coolant air from the turbine blade surface cause significantly different effects on turbine efficiency.

Since high turbine efficiency is important in most engine designs, an extensive research program is in progress at the Lewis Research Center to investigate both experimentally and analytically the effect of different means of coolant ejection on turbine efficiency as well as other aspects of turbine performance.

In previous investigations, several means of coolant ejection have been investigated. For instance, reference 3 reports the results of an experimental investigation of the effect on stator blade performance of coolant ejection from four spanwise rows of coolant holes located in or near the diffusion region on the suction surface at an angle of 35° to the blade surface with the axis of the holes parallel to the end walls. References 4 to 6 report the results of experimental and analytical investigations of the influence of turbine stator blade trailing-edge coolant ejection on turbine stator and stage performance. And references 7 to 10 report the results of experimental and analytical investigations of the effect of two types of stator blade transpiration discharge on turbine stator and stage performance. The results of the investigations of references 4 to 10 are summarized in reference 11.

The main conclusions of the investigations of references 3 to 10 were that (1) coolant flow discharged from the suction surface in or near the diffusion region at an angle of 35° to the blade surface would decrease the turbine work output at low coolant ejection velocities and increase the turbine work output at high coolant velocities, (2) coolant flow ejected from a trailing-edge slot parallel to the main stream significantly increased the turbine work output, and (3) coolant flow ejected over the complete blade surface at an angle normal to the blade surface contributed little or nothing to the turbine work output.

The investigation of this report is part of a continuing investigation of the effect of different means of stator blade full film cooling on turbine stator and stage performance. It concerns the effect on stator blade performance of coolant ejection from six spanwise rows of holes spaced along the pressure surface of the blading. The axes of the holes were located parallel to the end walls at various angles to the blade surface as dictated by cooling and aerodynamic considerations. The subject investigation may be considered an extension of the previously mentioned film cooling investigation of reference 3, which concerned the effect on stator performance of coolant ejection from four spanwise rows of coolant holes on the suction surface of the blading.

The testing for this report was conducted in a two-dimensional cascade. The temperature of the primary and coolant air were nearly the same, atmospheric air being used as the primary air.

In this investigation, the influence on stator blade performance of coolant discharge from each of the six single rows of coolant holes was first determined separately. Then the effect of multirow ejection was determined. In the multirow investigation, the combinations of coolant rows considered were the two rows nearest the blade leading edge, the three rows nearest the leading edge, etc. until all six rows were included.

The single and multirow tests were conducted at nominal ideal primary-air exit critical velocity ratios of approximately 0.5, 0.65, and 0.8. The range of coolant- to primary-air mass flow ratios investigated was from zero to about 3 percent from each coolant row.

The principal results are reported in terms of primary-air efficiency as a function of coolant flow rate. Primary-air efficiency is defined as the ratio of actual kinetic energy of the total flow to ideal kinetic energy of the primary flow only, and the coolant flow rate is defined as the ratio of coolant- to primary-air mass flow.

In order to determine if the coolant ejected from upstream holes affects the performance of coolant ejected from succeeding holes downstream, the primary-air efficiency results of the single-row tests were added and compared with the primary-air efficiency results of the multirow tests.

In addition to the principal results reported in the section RESULTS AND DISCUSSION, experimentally determined values of coolant hole discharge coefficients, which are of engineering interest, are also presented in appendix B.

APPARATUS, INSTRUMENTATION, AND PROCEDURE

Blading

A photograph of the test blading showing the six rows of pressure surface coolant holes is shown in figure 1. As indicated, the blading is hollow and of constant cross section. The blade profiles correspond to the mean section profile of the stator blade of reference 12, in which the blades are described in detail. Significant dimensions of the blading are span, 10.16 centimeters (4.0 in.); chord, 5.74 centimeters (2.26 in.); and pitch, 4.14 centimeters (1.63 in.).

The profile of the blading and the location, geometry, and numbering system of the coolant holes and rows are presented in figure 2 and table I. The axes of all coolant holes are parallel to the planes of the blade end surfaces. The diameter and pitch of the coolant holes in all six rows are 0.076 and 0.114 centimeter (0.030 and 0.045 in.), respectively. Other pertinent data concerning the coolant holes are listed in table I. (All symbols are defined in appendix A.)

Cascade

The blading was tested in the simple two-dimensional cascade shown in figure 3. There are 12 blades in the cascade; however, only the three blades near the center are cooled. Other details of the cascade are described in detail in reference 13. Primary (atmospheric) air enters the cascade inlet shown on the right in figure 3, and coolant air

enters the inside of the three hollow blades near the center of the cascade through the coolant manifold and associated piping. The survey probe actuator indicated in figure 3 operates a slide in which a multipurpose survey probe is mounted downstream of the blading. The coolant and primary flow passing through the blading is discharged from the cascade through exhaust piping attached to the circular base of the cascade.

Instrumentation

A calibrated multipurpose survey probe of the type shown in figure 4 was used to determine the angle, static pressure, and loss in total pressure downstream of the blading. (A detailed description of this type probe is given in ref. 13.) Coolant total pressure inside the blade p'_c was measured with a total-pressure probe having the sensing element of the probe located 2.54 centimeters (1.0 in.) from the blade end walls on the coolant manifold side. The circular sensing end of the probe faced the coolant flow entering the blading so that the total pressure inside the blade was measured as accurately as was practical.

Coolant flow was measured by using calibrated sharp-edged orifice plates of various sizes located in either a 2.54- or 5.08-centimeter (1.0- or 2.0-in.) orifice pipe. The orifice pipes, including instrumentation and orifice plates, all conformed to ASME specifications.

Static pressures on the blade pressure surface were determined from manometer board measurements of seven static-pressure taps spaced along the mean section of the blade pressure surface. All pressure data taken during survey tests were measured by using calibrated strain-gage transducers.

Test Procedure

When investigations for both single and multirow coolant discharge were conducted, three blades of the same profile with the same row or rows of coolant holes open were installed near the center of the cascade. Coolant air was then supplied to these blades only. Data were taken for only the center blade of the three test blades so that the measured data simulated data for a blade in a completely cooled blade row having adjacent blades of the same design and with the same flow conditions. Also, to eliminate the effect of end wall conditions on the measurements, data were taken at the mean section of the blading only.

To operate the test facility, primary (atmospheric) air is flowed through the cascade by use of the laboratory altitude exhaust system, which is piped to the cascade outlet. Desired primary-air pressure ratios across the blade row are maintained by regulation

of an exhaust control valve. Coolant airflow is provided by the laboratory combustion air system. Desired coolant flow rates were obtained by first setting the desired upstream orifice pressure with an upstream pressure regulator and then setting the desired pressure ratio across the orifice plate by regulating a throttling valve downstream of the orifice plate.

Before the blade survey testing was started, blade pressure-surface static pressures were determined from manometer board readings at set primary-air ideal exit critical velocity ratios of 0.50, 0.65, and 0.80.

To conduct survey tests, the desired primary-air set-point critical velocity ratio and coolant flow rate were established for the blading by regulation of the primary and coolant flow control valves. A survey was then made with the multipurpose probe across one blade pitch of the middle test blade to determine the downstream flow condition of the test blading. During the survey, all data, including survey data, coolant flow data, etc. were digitized and recorded on magnetic tape. Also during testing, pertinent survey data were monitored on x,y-recorders, and all data were monitored by teletype feedback from the laboratory data processing center.

The investigation of the test blading included survey tests with both single and multirow coolant ejection. Separate tests were first made with ejection from each of the six single rows. Then tests were made with coolant ejection from multiple coolant rows. The combination of multirow tests included the two coolant rows nearest the leading edge, the three rows nearest the leading edge, etc. until all six rows were included. Table II lists the multirow tests.

The survey investigations of both single and multirow coolant discharge were conducted at nominal values of ideal primary-air exit critical velocity ratio $(V/V_{cr})_{id,3}$ of 0.5, 0.65, and 0.8. For the single-row investigation, the range of coolant flow rates investigated was from zero to about 3 percent. For the multirow investigations, the range of coolant fractions investigated varied for the following reasons. With multirow discharge, the minimum practical value of coolant rate occurs when the total pressure inside the blade p'_c is a little higher than the blade surface pressure p_s of the coolant row nearest the leading edge of the blade. If the total pressure inside the blade is lower than the blade surface pressure of the coolant row nearest the leading edge, primary air flows abnormally into the interior of the blade through the row nearest the leading edge and out coolant rows farther downstream. Under these conditions, a portion of the blade surface near the leading edge would, of course, not be film-cooled. The minimum coolant flow rates for multirow ejection were determined by this consideration, and the maximum coolant flow rates were determined by the number of coolant rows open with the total pressure inside the blade limited to 13.9 newtons per square centimeter (20 lb/in.² abs).

Calculation Procedure

The general procedure for computing the test results was as follows: Coolant flow rates were computed by the method specified in the ASME code for sharp-edged orifices. Local values of mass flow, momentum, flow angle, static pressure, and kinetic energy at each data point included in the survey were then computed. The local values of mass flow, momentum, etc. were next integrated at the measuring station. Then, with conservation of mass and momentum assumed, the integrated values at the measuring station were equated to the same quantities at the hypothetical-aftermixed downstream station. These equations were then solved simultaneously to obtain the aftermixed flow conditions. (Equations for the survey data calculation procedure may be found in ref. 14.) With the aftermixed flow conditions known, primary-air efficiency, as well as other results of interest, could be computed at fully mixed flow conditions.

Efficiency. - There are a number of efficiency expressions commonly used to describe the performance of high-temperature turbines requiring coolant. For cold aerodynamic tests with no internal inserts to duplicate actual hot engine heat transfer or pressure drop, the selection becomes arbitrary. The major parameter studied in the aerodynamic tests of this report was the effect of ejected coolant on the output kinetic energy of the combined flow (primary plus coolant). Therefore, primary efficiency was selected because it was felt to be the most direct form of efficiency with which to investigate changes in output energy as affected by adding coolant. Primary efficiency relates the actual kinetic energy of the total flow to the ideal energy of only the primary flow and is expressed as

$$\eta_p = \frac{w_t V_3^2}{w_p V_{p, id}^2} \quad (1)$$

which in terms of isolated flows is equivalent to

$$\eta_p = \frac{w_p V_p^2 + w_c V_c^2}{w_p V_{p, id}^2} \quad (2)$$

Equation (1) was used to compute experimental results.

Thermodynamic efficiency is the same as primary efficiency except that the ideal energy of the coolant flow is included in the denominator. Because the stator blades have fixed holes, the only way to vary coolant flow is to vary the blade cavity pressure, which in turn varies the ideal energy of the coolant. The major reason primary

efficiency was selected over thermodynamic efficiency, then, was that it reduces the number of variables to consider when studying the effect of coolant on output energy. If primary efficiency increases with coolant addition, the coolant contributes energy at the exit. If efficiency remains unchanged, the net effect is that the coolant adds no energy and the primary flow energy remains unchanged. If primary efficiency decreases, the net effect is that (1) the coolant adds no energy and (2) the presence of the coolant also reduces the efficiency of the primary flow.

Prediction of multirow performance by addition of single-row data. - The manner of considering the effect of coolant on efficiency for both single-row (SR) and multirow (MR) tests is to plot the fractional change in primary efficiency $\Delta\eta_p/\eta_0$ against coolant fraction y , where $\Delta\eta_p = \eta_p - \eta_0$ and η_0 is the efficiency of the blade row with no coolant. The model used is similar to that used in the isolated-flow analysis of reference 5, where it is assumed that the efficiency of the primary air is unaffected by the coolant. Although it is recognized that this is not true, it enables the results to be interpreted consistently with the use of primary-air efficiency (see eq. (2)). That is, all changes in efficiency are attributed to the coolant flow.

In adding the single-row data to predict multirow performance, the following assumptions are made concerning each given single-row condition applied to multirow conditions:

- (1) Constant $w_{c,SR}$ for same cavity pressure
- (2) Constant $V_{c,SR}$ (no change in loss)
- (3) Constant $V_{p,id}$ (same setting condition)
- (4) Constant V_p (no change in efficiency of primary air)

With these assumptions, the change in efficiency for the multirow case in terms of single-row conditions is calculated as follows: Equation (2) is rewritten (with assumptions (3) and (4)) as

$$\eta_p = \eta_0 + \frac{w_c V_c^2}{w_p V_{p,id}^2} \quad (3)$$

or

$$w_c V_c^2 = \Delta\eta_p w_p V_{p,id}^2 \quad (4)$$

where η_0 is the efficiency with no coolant and is constant. For multirow conditions, assume rows 1 and 2 open (indicated by the subscript 1+2). Rewriting equation (3) with assumptions (1) and (2) gives

$$\eta_{p, 1+2} = \eta_0 + \frac{w_{c, 1+2} V_{c, 1+2}^2}{w_{p, 1+2} V_{p, id}^2} = \eta_0 + \frac{w_{c, 1} V_{c, 1}^2 + w_{c, 2} V_{c, 2}^2}{w_{p, 1+2} V_{p, id}^2}$$

Then

$$\Delta\eta_{p, 1+2} = \frac{\Delta\eta_{p, 1} w_{p, 1} V_{p, id}^2 + \Delta\eta_{p, 2} w_{p, 2} V_{p, id}^2}{w_{p, 1+2} V_{p, id}^2} \quad (5)$$

and

$$\left(\frac{\Delta\eta_p}{\eta_0}\right)_{1+2} = \frac{w_{p, 1}}{w_{p, 1+2}} \left(\frac{\Delta\eta_p}{\eta_0}\right)_1 + \frac{w_{p, 2}}{w_{p, 1+2}} \left(\frac{\Delta\eta_p}{\eta_0}\right)_2$$

where subscripts 1 and 2 refer to single-row conditions of row 1 and row 2, and the subscript 1+2 refers to multirow conditions where rows 1 and 2 are open. For the general multirow case with n rows open,

$$\left(\frac{\Delta\eta_p}{\eta_0}\right)_{MR} = \sum_{SR=1}^{SR=n} \frac{w_{p, SR}}{w_{p, MR}} \left(\frac{\Delta\eta_p}{\eta_0}\right)_{SR} \quad (6)$$

Similarly, the summation of coolant fractions (with assumption (1)) is as follows: Again with rows 1 and 2 assumed open,

$$y_{1+2} = \frac{w_{c, 1} + w_{c, 2}}{w_{p, 1+2}} \quad (7)$$

or

$$y_{1+2} = \frac{w_{c, 1}}{w_{p, 1}} \frac{w_{p, 1}}{w_{p, 1+2}} + \frac{w_{c, 2}}{w_{p, 2}} \frac{w_{p, 2}}{w_{p, 1+2}}$$

and

$$y_{1+2} = \left(\frac{w_{p,1}}{w_{p,1+2}} \right) y_1 + \left(\frac{w_{p,2}}{w_{p,1+2}} \right) y_2 \quad (8)$$

For the general case

$$y_{MR} = \sum_{SR=1}^{SR=n} \left(\frac{w_{p,SR}}{w_{p,MR}} \right) y_{SR} \quad (9)$$

If the amount of primary flow did not change with coolant, inspection of equations (6) and (9) indicates that the change in efficiency and summation of coolant fractions would simply be

$$\left(\frac{\Delta \eta_p}{\eta_0} \right)_{MR} = \sum_{SR=1}^{SR=n} \left(\frac{\Delta \eta_p}{\eta_0} \right)_{SR} \quad (10)$$

and

$$y_{MR} = \sum_{SR=1}^{SR=n} y_{SR} \quad (11)$$

Accuracy of Results

Concerning the accuracy of the results, statistical evidence obtained from many tests by several investigators using this same facility indicates the maximum probable error in primary-air efficiency is about ± 0.25 percent for uncooled blading. The exact causes of the error are not known; however, it is the speculation of the investigators that the error could result from several causes, such as measurement inaccuracy, actual changes in the efficiency of the same blading due to fluctuations in flow or fluctuations in location of the boundary-layer flow transition point from laminar to turbulent on the blade surfaces, or temporary collection of foreign material on either the blade or the survey probe surfaces during testing.

RESULTS AND DISCUSSION

The results of the investigation are presented in two sections. The first section includes the experimentally determined stator efficiencies of (1) the six rows of coolant holes on the pressure surface tested individually and (2) multirow tests using various combinations of coolant row holes. The second section compares the experimentally determined stator efficiencies of the multirow tests with those predicted by adding the results of the single-row tests.

Single-Row and Multirow Experimental Results

The performance of the stator with single-row and multirow coolant ejection is given in terms of changes in primary-air efficiency with coolant flow. As mentioned in the section Efficiency, primary-air efficiency was used rather than thermodynamic efficiency because it is simpler to study factors that influence the output energy of the flow if the varying ideal energy of the coolant does not have to be considered.

Single-row experimental performance. - The single-row variation in primary-air efficiency for each of the six single-row ejection tests is shown in figure 5 over a range of coolant fractions from 0 to 0.04. Data are shown for each configuration for ideal exit velocity ratios of 0.5, 0.65, and 0.8. The efficiency of the single configurations with no coolant varied from about 0.97 to 0.98 over the range of Mach numbers tested. As coolant was added, two effects could be observed. First, the trend of increasing efficiency with additional coolant was similar for all configurations. Second, Mach number had very little effect on change in efficiency, especially if the efficiency was normalized to each particular zero-coolant-flow case. Such a relation is shown in figure 6.

The fractional change in efficiency compared to zero-coolant efficiency $\Delta\eta_p/\eta_0$ is shown in figure 6 as a function of coolant fraction for the six single-row configurations tested and was obtained by averaging the data from figure 5 for all Mach numbers tested. As expected, the trends were similar for all configurations. An increase in the slope of the curves with increasing coolant fractions would be expected because higher cavity pressures (and ideal coolant energy) would be required to eject more coolant through fixed holes. When the cavity pressure is equal to the inlet pressure of the primary air, the ideal energies of the coolant and primary air are equal. For this condition, test results indicated that the coolant ejection from rows 1 to 6 ranged from about 0.5 to 1.5 percent of the primary flow. The corresponding efficiency increases from figure 6 ranged from about 0.4 to 1.2 percent. In other words, for a constant efficiency of the primary air, about 80 percent of the ideal energy of the coolant was converted into net useful output energy at the exit of the blade row.

Multirow experimental performance. - The variation in efficiency with coolant flow for the stator with multirow coolant ejection from the pressure surface is shown in figures 7 and 8. The vertical marks on the curves indicate the minimum amount of coolant where coolant was being ejected from all holes. For lower coolant rates, the cavity pressure would have been less than the primary stream pressure at row 1, and inflow of primary air through row 1 coolant holes would have resulted.

The multirow results in figure 7 are similar to the single-row results of figure 5 in the following respects. There was very little Mach number effect for the range of ideal exit velocity ratio $(V/V_{cr})_{3, id}$ indicated, and there was a substantial increase in output energy (primary efficiency) resulting from the coolant. Also, there was the same expected increase in slope resulting from the increased cavity pressure (and ideal energy of the coolant) required to increase the coolant flow.

The change in primary efficiency with coolant for multirow ejection is seen more clearly in figure 8, where the average data from figure 7 for each multirow configuration tested are shown. As indicated, all of the data for all configurations tested fell in a narrow band. For given coolant fractions below 0.08, there was a slight increase in efficiency as number of coolant holes decreased. This could have been expected since, for the same coolant fraction, fewer holes require higher cavity pressures and higher coolant velocities. This trend did not hold for coolant fractions above 0.08, where the increase in efficiency for the six-row configuration was higher than that for the five-row configuration. However, considering the measuring accuracy and the limitations of a two-dimensional cascade, figure 8 indicates that an average curve through the data would represent very closely the change in primary efficiency with coolant fraction for the stator blade tested. That is, the output energy is dependent primarily on the amount of coolant ejected and is only slightly affected by the number or location of holes and Mach number.

Comparison of Additive Single-Row Data With Multirow Data

In order to determine if the coolant ejected from upstream holes affects the performance of coolant ejected from succeeding holes downstream, the results of the single-row tests were added and compared with the multirow test results. The effect of cavity pressure on coolant flow for the various rows of holes is presented first. Next, the effect of the coolant flow on primary flow is given. Finally, the results of the single-row tests are added and compared with the results of the multirow tests.

Effect of cavity pressure on coolant flow. - The amount of coolant ejected from each row of holes as a function of cavity pressure is presented in figure 9, where coolant fraction y is plotted against a pressure coefficient k_p which relates the total - to

static-pressure drop available to the coolant to that of the primary air. All the curves are nearly parallel except that for row 1, which turns downward, probably because row 1 was close to the leading edge stagnation point. The extrapolation of the curve for row 1 would indicate that coolant flow decreased to zero at a pressure coefficient k_p of about 0.9. This was the value used to determine the vertical marks of minimum coolant flow referred to in connection with figures 7 and 8. Although the curves in figure 9 are indicated to be for an ideal exit velocity ratio of 0.65, they are valid for $(V/V_{cr})_{id,3}$ values of 0.5 and 0.8 also.

Effect of coolant flow on primary flow. - The reduction in primary flow caused by the addition of coolant is shown in figures 10 and 11 for single-row and multirow ejection, respectively. The curves shown were averaged from data obtained at all Mach numbers. As indicated in figure 11, an averaged single curve was used for all multirow data. The reduction in primary flow was significant. For example, figure 11 shows that a coolant addition of 0.02 reduced primary flow by 0.04. The effect lessened as more coolant was added and resulted in primary-flow reductions of 0.06 and 0.10 at coolant fractions of 0.04 and 0.10, respectively. For these tests, the inlet temperatures of both the coolant and primary air were the same. For an actual hot turbine where temperature ratios (primary inlet to coolant inlet) up to 3 may be encountered, the density of the coolant at the ejection point will be much higher than that of the primary air. Depending on the amount of heat transfer between the primary and coolant air, lower volumes may be required by the coolant and the effect of reduction in primary airflow may be lessened.

Predicted multirow performance. - In order to add single-row data to predict multirow results, values of k_p were selected. For a given value of k_p , the amount of coolant from each row was selected from figure 9. These values of y were then used to determine corresponding values of $\Delta\eta_p/\eta_0$ from figure 6 for each row. If the primary airflow w_p did not change with coolant addition, the multirow predicted performance was determined by simply adding the single-row y and $\Delta\eta_p/\eta_0$ values for the case in question (eqs. (10) and (11)). However, as indicated in the section Calculation Procedure, individual single-row hole values of both y_{SR} and $(\Delta\eta_p/\eta_0)_{SR}$ must be corrected for changes in primary flow that result from adding coolant. Figures 10 and 11 were used in conjunction with figures 9 and 6 to predict multirow performance from single-row data by means of equations (6) and (9).

Figure 12 shows the predicted multirow performance obtained by adding the single-row data. The curves are very similar to the experimental multirow results of figure 8. The trend of slight increase in efficiency with fewer rows for a given coolant fraction persists over the entire range of coolant fractions. As with the experimental multirow data, a single averaging curve would very closely represent the predicted efficiencies for all configurations tested over the entire range of coolant fractions.

Comparison of predicted and experimental multirow performance. - A comparison of predicted (additive single-row data) with experimental multirow efficiency variation

with coolant fraction is shown in figure 13. Single averaging curves were obtained from figures 8 (experimental) and 12 (predicted) and show very close agreement over the entire range of coolant flows. Figure 13 indicates a maximum difference of less than 0.01 in efficiency for coolant fractions up to 0.15.

Figure 13 also shows that, for the stator blade tested, coolant ejected from a row of holes on the pressure surface apparently did not affect the performance of coolant ejected from holes farther downstream on the pressure surface.

SUMMARY OF RESULTS

The influence on stator blade performance of coolant discharge from each of six individual rows of coolant holes on the pressure surface was determined experimentally. Multirow combinations of two, three, four, five, and six rows of holes were also tested. The results of the multirow tests were then compared with predicted multirow performance obtained by adding the results of the single-row tests. The tests were conducted in a two-dimensional cascade where the temperature of the coolant was equal to the inlet temperature of the primary air. Each configuration was tested over a range of coolant flows at ideal primary-air exit critical velocity ratios of 0.5, 0.65, and 0.8. The results are summarized as follows:

1. For the blade tested, the change in primary efficiency was dependent primarily on the amount of coolant added and was essentially independent of the number or location of coolant holes and the Mach number.

2. A significant portion of the ideal energy of the coolant resulted in useful kinetic energy at the exit of the blade row. When the blade cavity pressure (coolant supply) was equal to the inlet pressure of the primary flow, about 80 percent of the ideal coolant energy was measured at the blade exit as a net increase in kinetic energy output.

3. The output energy from single-row holes was additive. Excellent agreement was obtained between measured multirow coolant ejection performance and predicted multirow performance obtained by adding measured single-row data. Apparently flow from a row of holes on the pressure surface did not affect the performance of coolant flow ejected from holes downstream on the pressure surface.

Lewis Research Center,
National Aeronautics and Space Administration,
Cleveland, Ohio, January 24, 1974,
501-24.

APPENDIX A

SYMBOLS

A	area, m^2 ; ft^2
C_D	discharge coefficient, ratio of actual flow to ideal flow
D	diameter of coolant hole, cm; in.
k_p	pressure coefficient
L	coolant hole length, cm; in.
L_{pr}	pressure-surface length from leading edge to trailing edge (see fig. 2), cm; in.
n	number of coolant rows open
p	absolute pressure, N/m^2 ; lbf/ft^2
Re	Reynolds number
T	absolute temperature, K; $^{\circ}R$
V	absolute velocity, m/sec; ft/sec
w	mass flow rate, kg/sec; lbm/sec
x	local position along pressure surface from leading edge (see fig. 2), cm; in.
y	coolant fraction, w_c/w_p
β	angle between coolant hole centerline and local blade surface tangent, deg
η_p	primary-air efficiency, ratio of kinetic energy of total flow to ideal kinetic energy of primary flow only
η_0	blade-row efficiency with no coolant flow
μ	viscosity, $(N)(sec)/m^2$; $lbf/(sec)(ft)$
ρ	density, kg/m^3 ; lbf/ft^3

Subscripts:

c	coolant flow
cr	Mach 1
h	coolant hole
id	ideal quantity corresponding to isentropic process
MR	multiple rows of coolant holes open
p	primary flow

- SR single row of coolant holes open
- s local blade surface
- t total flow
- 0 no coolant flow
- 1 station at blade row inlet
- 3 station at blade exit, where flow conditions are assumed uniform

Superscript:

- ' total state

APPENDIX B

COOLANT HOLE DISCHARGE COEFFICIENTS

This appendix presents the coolant hole discharge coefficients for each of the six coolant hole configurations tested. The discharge coefficients are presented as a function of both ideal coolant hole Reynolds number and primary-air exit critical velocity ratio.

The discharge coefficients are, of course, the ratio of the actual to the ideal flow through the coolant hole. Thus,

$$C_{D,h} = \frac{w_{c,h}}{(\rho V)_{id,h} A_h} \quad (B1)$$

The actual coolant flow per hole $w_{c,h}$ was determined by using sharp-edged-orifice data.

The upstream flow conditions used for the determination of the ideal density and velocity at the exit of the hole were obtained from the measured total pressure and temperature inside the blade p'_c and T'_c , and the downstream flow conditions used for the determination of the ideal density and velocity at the exit of the hole were obtained from the measured blade surface static pressure p_s at the location of the coolant hole x_h .

The ideal Reynolds numbers based on the hole diameter were computed from the standard relation

$$Re_{id,h} = \frac{(\rho V D)_{id,h}}{\mu} \quad (B2)$$

Figure 14 presents the coolant hole discharge coefficients as a function of both ideal Reynolds number and ideal primary-air exit critical velocity ratio for the six coolant rows. In addition, in figure 15 the ratios of blade surface static pressure to inlet total pressure at the different coolant row locations are presented as a function of blade surface length and primary-air ideal exit critical velocity ratio. (These pressure ratios are presented for completeness in case the reader might wish to use the experimental data for other calculations.)

In figure 14, the discharge coefficients are shown to vary with Reynolds number and primary-air critical velocity ratio. The maximum discharge coefficients, at the maximum Reynolds number considered, varied from about 0.65 to 0.8 for the different hole configurations. In general, for all hole configurations, the discharge coefficients decreased with decreasing Reynolds number. At the higher Reynolds numbers, the

coefficients were, in general, affected only slightly by primary-air critical velocity; however, as the Reynolds number decreased from the maximum considered, the coefficients for all configurations were affected to some degree by primary-air critical velocity ratio. The general trend of coefficients at the lower Reynolds numbers is to decrease with increasing primary-air critical velocity ratio.

REFERENCES

1. Hartsell, J. E. : Prediction of Effects of Mass-Transfer Cooling on the Blade Row Efficiency of Turbine Airfoils. AIAA Paper No. 72-11, January 1972.
2. Prust, Herman W. , Jr. : An Analytical Study of the Effect of Coolant Flow Variables on the Kinetic Energy Output of a Cooled Turbine Blade Row. AIAA Paper No. 72-12, January 1972.
3. Brown, Douglas B. ; and Henlon, Ronald M. : Cold-Air Aerodynamic Study in a Two-Dimensional Cascade of a Turbine Stator Blade with Suction-Surface Film Cooling. NASA TM X-2685, 1973.
4. Whitney, Warren J. ; Szanca, Edward M. ; and Behning, Frank P. : Cold-Air Investigation of a Turbine with Stator-Blade Trailing-Edge Coolant Ejection. I - Overall Stator Performance. NASA TM X-1901, 1969.
5. Whitney, Warren J. : Comparative Study of Mixed- and Isolated-Flow Methods for Cooled-Turbine Performance Analyses. NASA TM X-1572, 1968.
6. Szanca, Edward M. ; Schum, Harold J. ; and Prust, Herman W. , Jr. : Cold-Air Investigation of a Turbine with Stator-Blade Trailing-Edge Coolant Ejection. III - Overall Stage Performance. NASA TM X-1974, 1970.
7. Prust, Herman W. , Jr. ; Schum, Harold J. ; and Szanca, Edward M. : Cold-Air Investigation of a Turbine with Transpiration-Cooled Stator Blades. I - Performance of Stator with Discrete Hole Blading. NASA TM X-2094, 1970.
8. Szanca, Edward M. ; Schum, Harold J. ; and Behning, Frank P. : Cold-Air Investigation of a Turbine with Transpiration-Cooled Stator Blades. II - Stage Performance with Discrete Hole Stator Blades. NASA TM X-2133, 1970.
9. Behning, Frank P. ; Prust, Herman W. , Jr. ; and Moffitt, Thomas P. : Cold-Air Investigation of a Turbine with Transpiration-Cooled Stator Blades. III - Performance of Stator with Wire-Mesh Shell Blading. NASA TM X-2166, 1971.
10. Behning, Frank P. ; Schum, Harold J. ; and Szanca, Edward M. : Cold-Air Investigation of a Turbine with Transpiration-Cooled Stator Blades. IV - Stage Performance with Wire-Mesh Shell Stator Blading. NASA TM X-2176, 1971.
11. Moffitt, Thomas P. ; Prust, Herman W. , Jr. ; Szanca, Edward M. ; and Schum, Harold J. : Summary of Cold-Air Tests of a Single-Stage Turbine with Various Stator Cooling Techniques. NASA TM X-52968, 1971.

12. Whitney, Warren J. ; Szanca, Edward M. ; Moffitt, Thomas P. ; and Monroe, Daniel E. : Cold-Air Investigation of a Turbine for High-Temperature-Engine Application. I - Turbine Design and Overall Stator Performance. NASA TN D-3751, 1967.
13. Stabe, Roy G. : Design and Two-Dimensional Cascade Test of Turbine Stator Blade with Ratio of Axial Chord to Spacing of 0.5. NASA TM X-1991, 1970.
14. Goldman, Louis J. ; and McLallin, Kerry L. : Cold-Air Annular-Cascade Investigation of Aerodynamic Performance of Cooled Turbine Vanes. I - Facility Description and Base (Solid) Vane Performance. NASA TM X-3006, 1974.

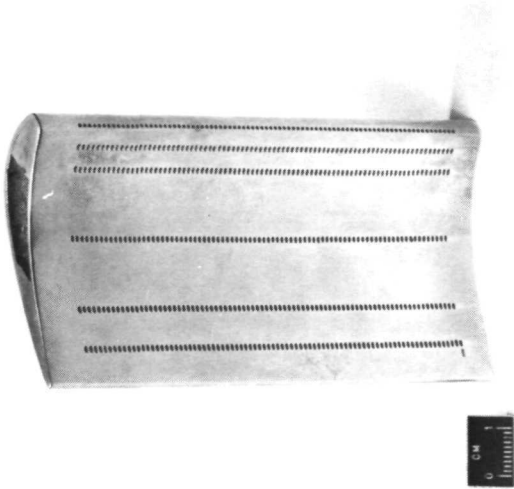
TABLE I. - COOLANT HOLE DATA

Coolant row	Percent of blade surface length, $(x/L_{pr}) \times 100$	Angle of coolant hole axis with blade surface, β , deg	Length to diameter ratio of coolant hole, L/D
1	3.5	90	2.2
2	12.0	34	3.7
3	20.0	33	3.3
4	45.0	35	3.3
5	70.0	33	3.3
6	85.0	34	3.3

TABLE II. - ROWS INCLUDED IN

MULTIROW COOLANT TESTS

Multirow configuration	Coolant rows included
1	1, 2
2	1 to 3
3	1 to 4
4	1 to 5
5	1 to 6



C-73-2665

Figure 1. - Blade tested.

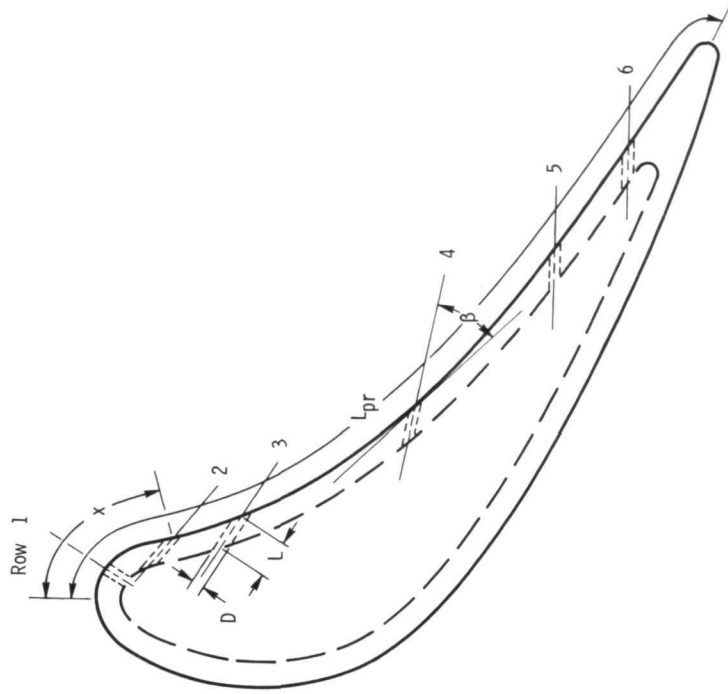


Figure 2. - Cross-sectional sketch of cooled blade.

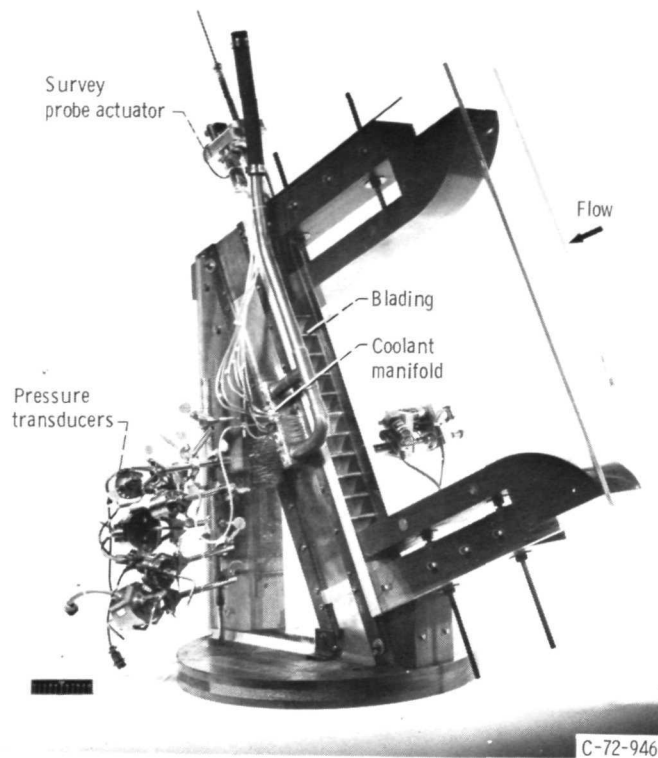


Figure 3. - Stator blade cascade.

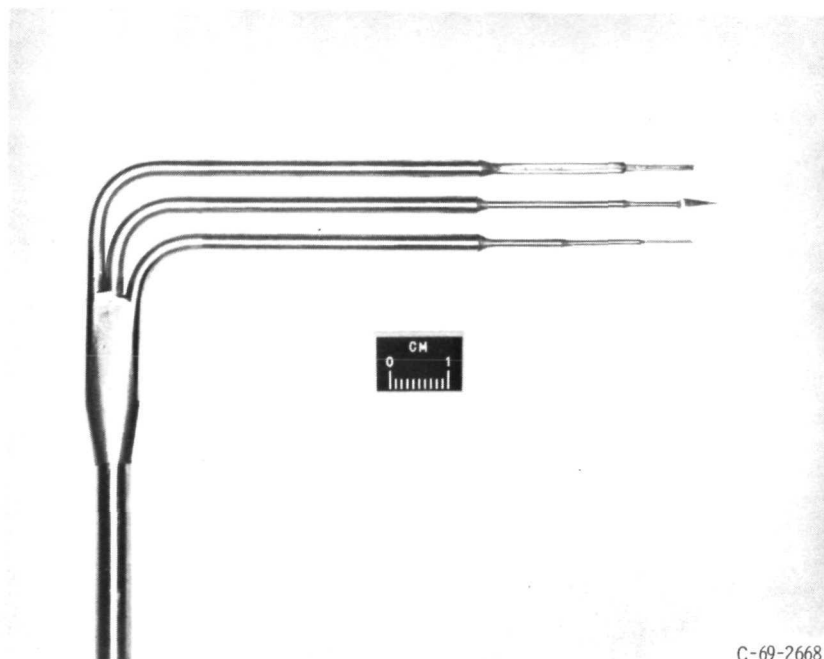


Figure 4. - Survey probe.

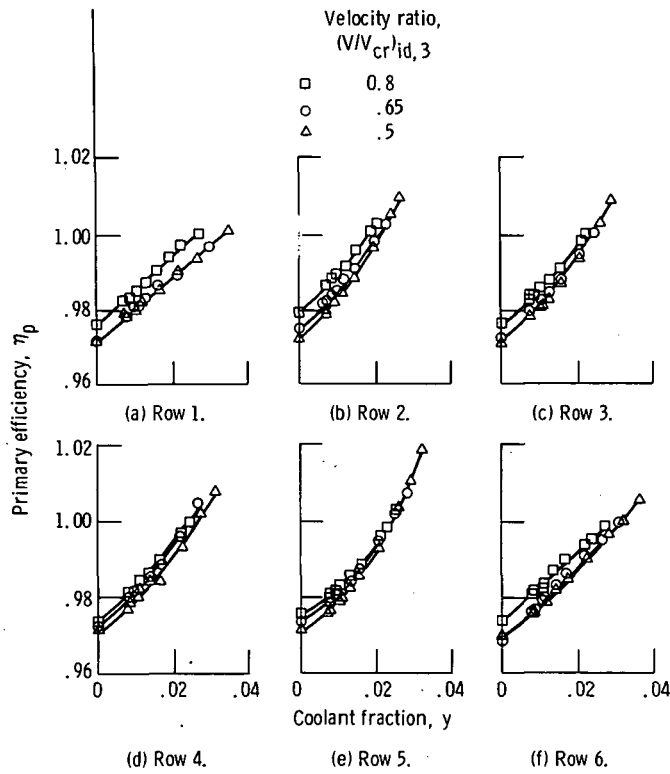


Figure 5. - Single-row variations in primary efficiency with coolant fraction and Mach number.

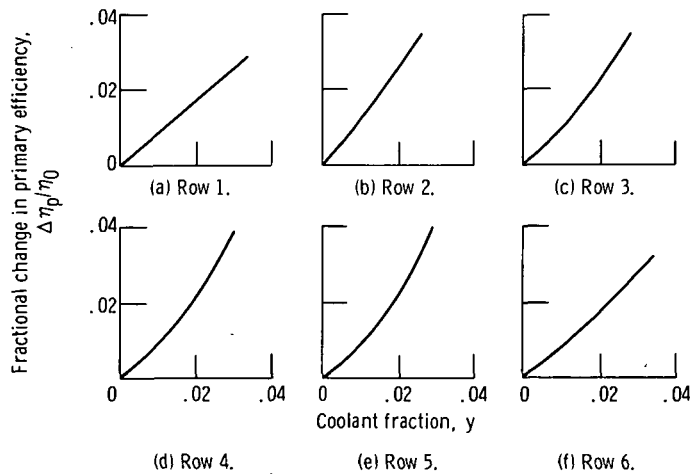


Figure 6. - Single-row fractional change in primary efficiency with coolant fraction. Data averaged from figure 5 for Mach number.

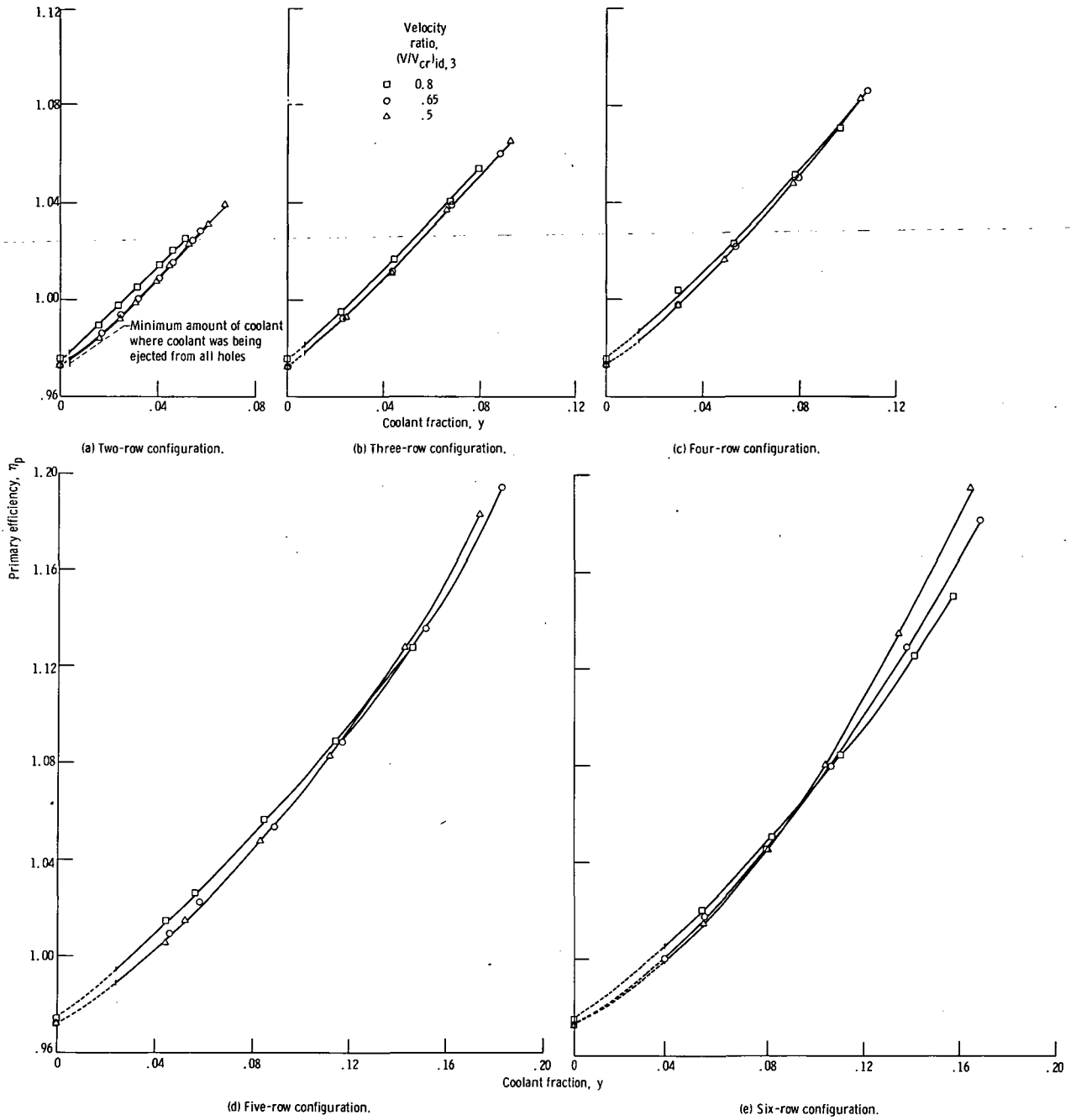


Figure 7. - Multirrow variation in primary efficiency with coolant fraction and Mach number.

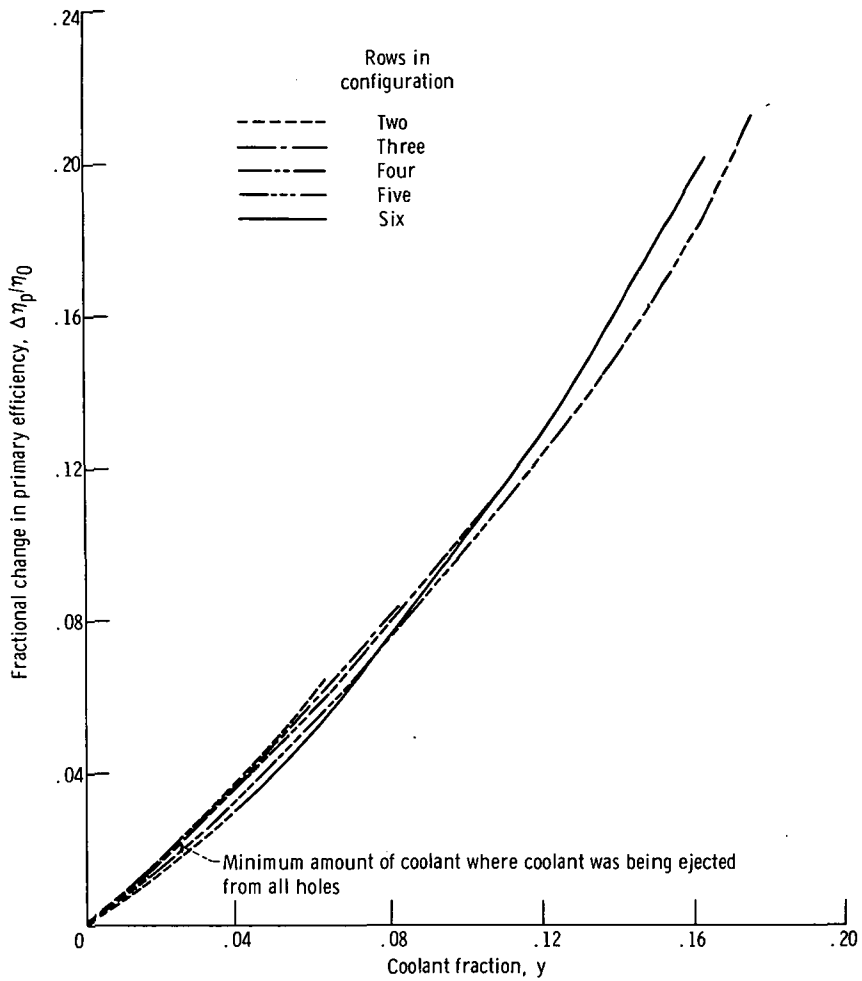


Figure 8. - Multirow fractional change in primary efficiency with coolant fraction. Data averaged from figure 7 for Mach number.

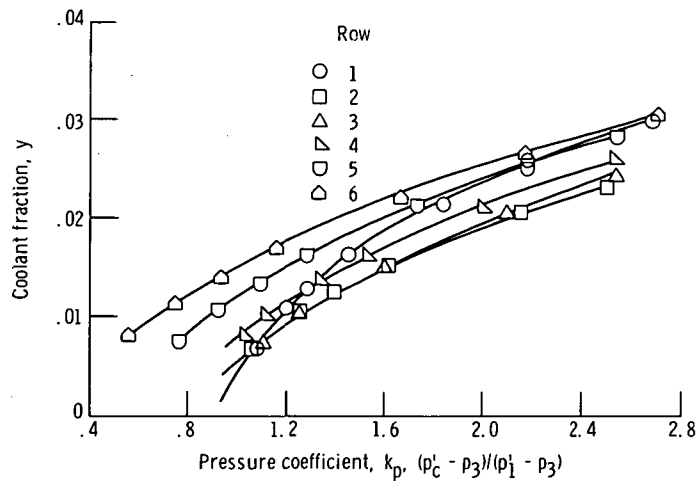


Figure 9. - Single-row coolant fraction as function of inlet coolant- to primary-air pressure coefficient. Velocity ratio, 0.65.

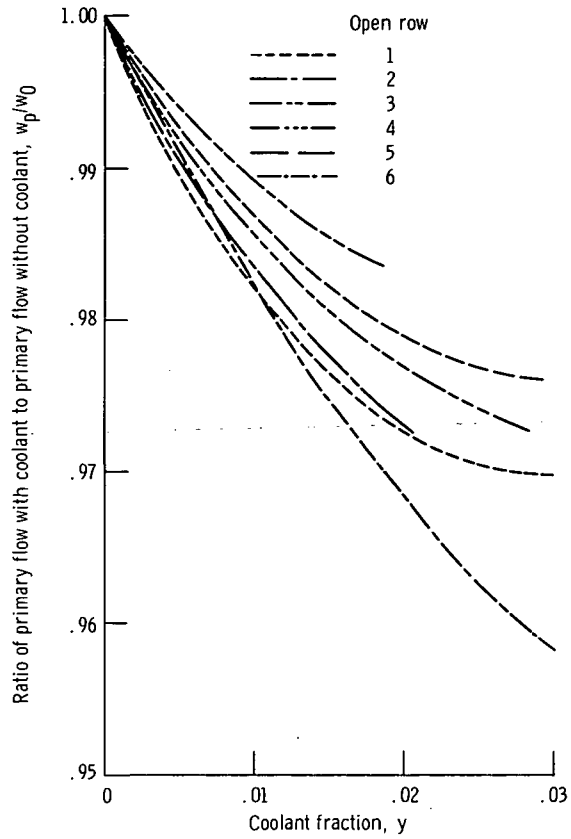


Figure 10. - Effect of coolant flow on primary flow for individual coolant rows opened. Data averaged for all Mach numbers.

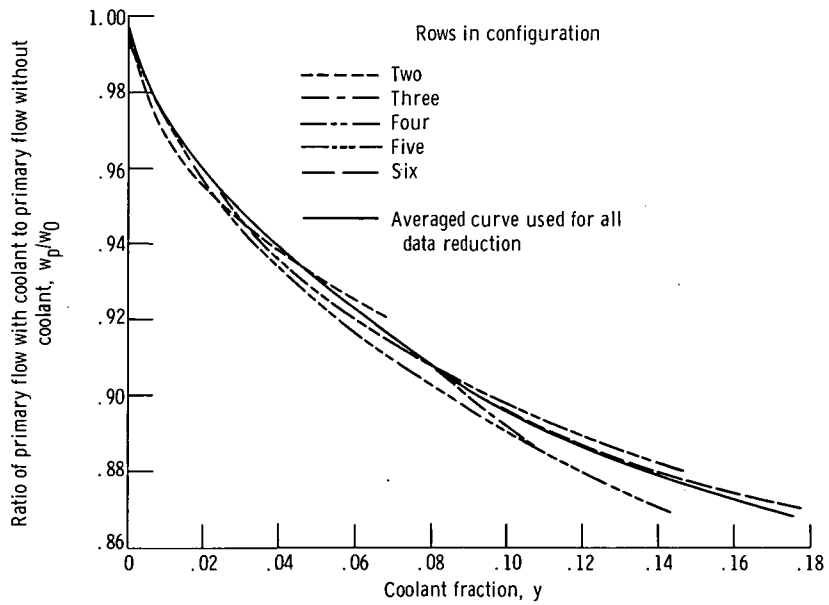


Figure 11. - Effect of coolant flow on primary flow for multirow tests.

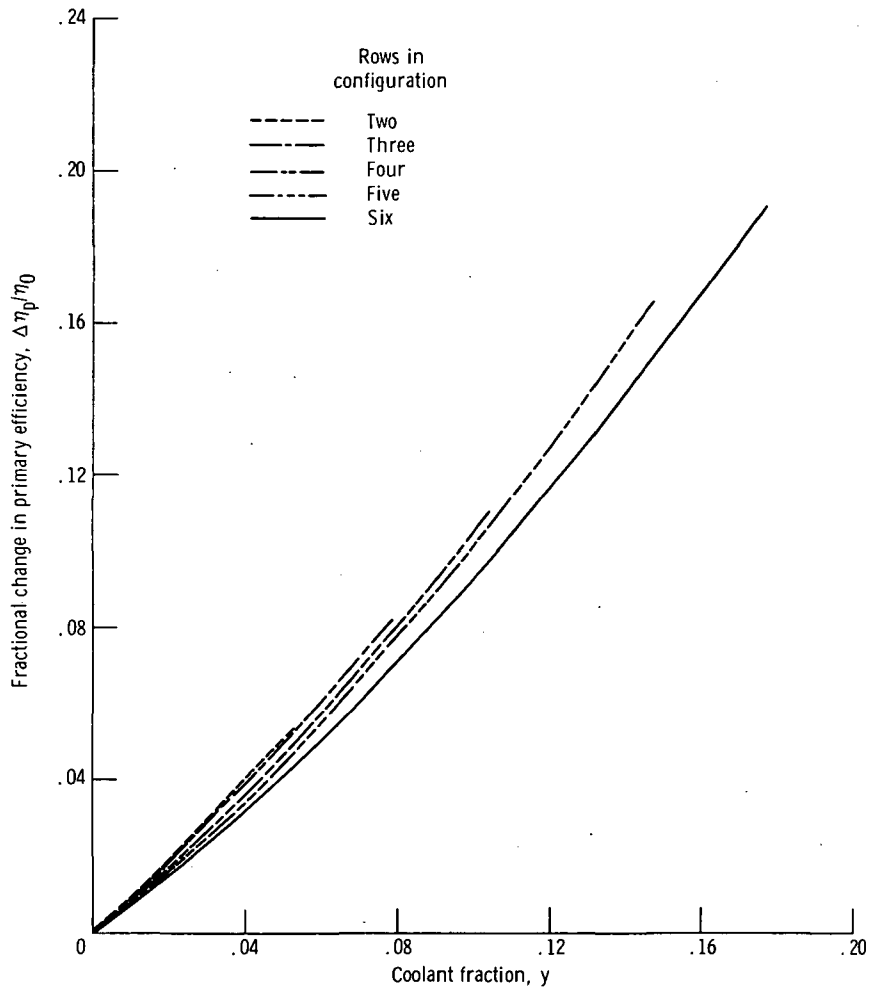


Figure 12. - Predicted change in performance of pressure-side multirow stator determined by adding single-row performance data.

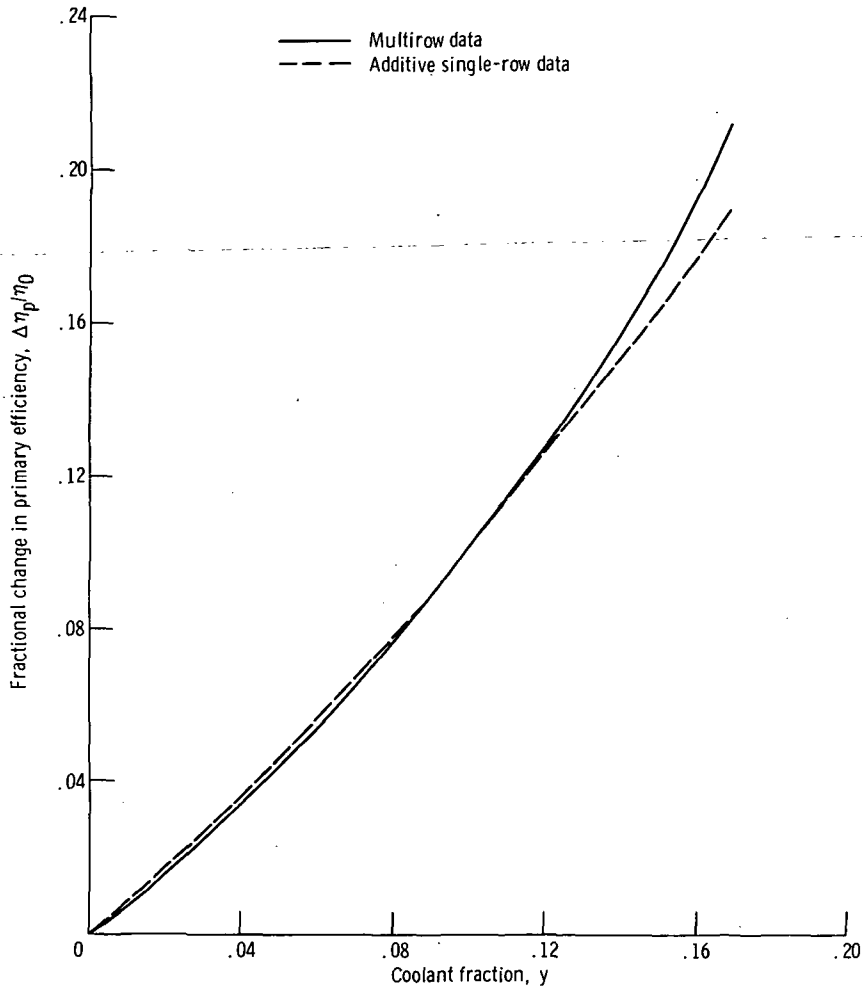


Figure 13. - Comparison of multirow data with additive single-row data for pressure side. Data averaged for all coolant row configurations and for all-Mach numbers tested.

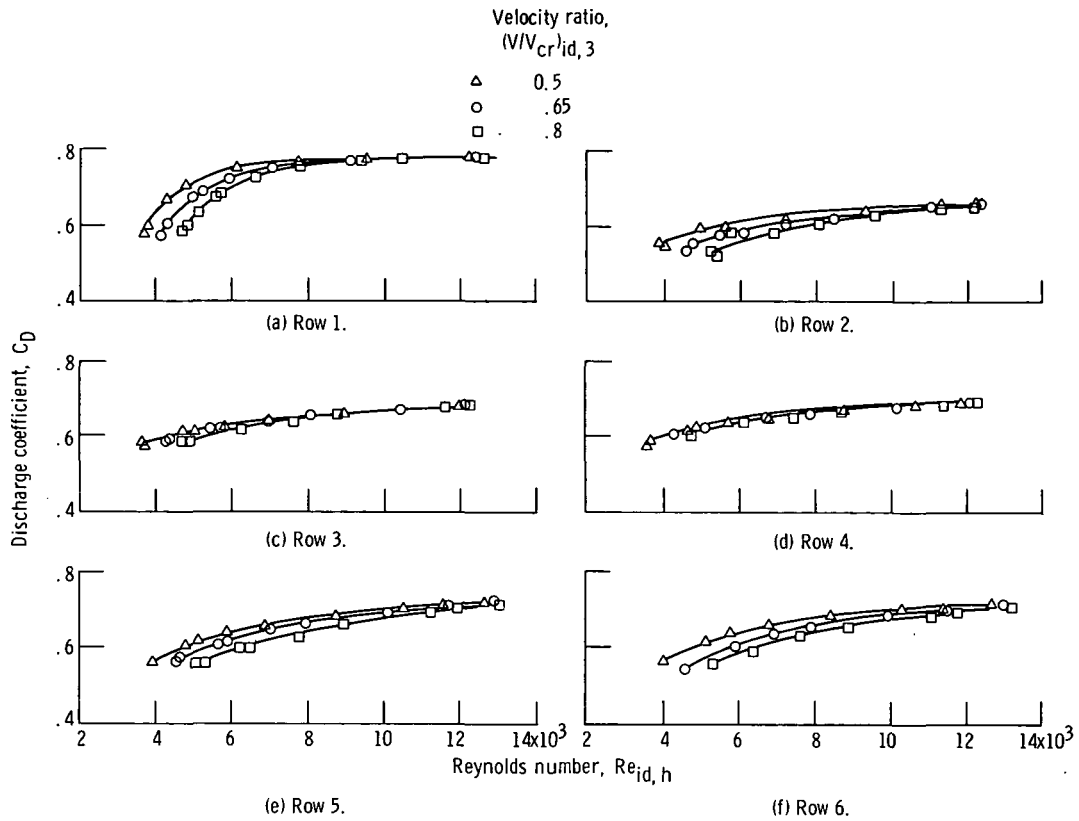


Figure 14. - Discharge coefficient of pressure-side coolant holes based on ideal Reynold's number of flow through holes.

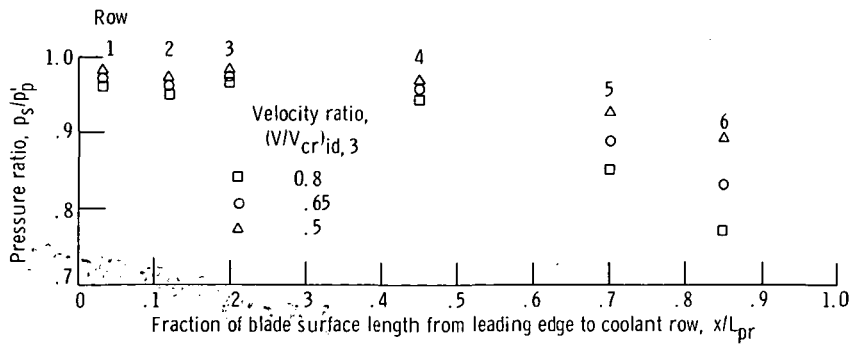


Figure 15. - Local coolant row pressure-surface static pressure as function of critical velocity ratio and blade surface length.

Page Intentionally Left Blank



POSTMASTER: If Undeliverable (Section 158
Postal Manual) Do Not Return

"The aeronautical and space activities of the United States shall be conducted so as to contribute . . . to the expansion of human knowledge of phenomena in the atmosphere and space. The Administration shall provide for the widest practicable and appropriate dissemination of information concerning its activities and the results thereof."

—NATIONAL AERONAUTICS AND SPACE ACT OF 1958

NASA SCIENTIFIC AND TECHNICAL PUBLICATIONS

TECHNICAL REPORTS: Scientific and technical information considered important, complete, and a lasting contribution to existing knowledge.

TECHNICAL NOTES: Information less broad in scope but nevertheless of importance as a contribution to existing knowledge.

TECHNICAL MEMORANDUMS: Information receiving limited distribution because of preliminary data, security classification, or other reasons. Also includes conference proceedings with either limited or unlimited distribution.

CONTRACTOR REPORTS: Scientific and technical information generated under a NASA contract or grant and considered an important contribution to existing knowledge.

TECHNICAL TRANSLATIONS: Information published in a foreign language considered to merit NASA distribution in English.

SPECIAL PUBLICATIONS: Information derived from or of value to NASA activities. Publications include final reports of major projects, monographs, data compilations, handbooks, sourcebooks, and special bibliographies.

TECHNOLOGY UTILIZATION PUBLICATIONS: Information on technology used by NASA that may be of particular interest in commercial and other non-aerospace applications. Publications include Tech Briefs, Technology Utilization Reports and Technology Surveys.

Details on the availability of these publications may be obtained from:

SCIENTIFIC AND TECHNICAL INFORMATION OFFICE

NATIONAL AERONAUTICS AND SPACE ADMINISTRATION

Washington, D.C. 20546